TRACER AND DARCY-BASED IDENTIFICATION OF SUBSURFACE FLOW, BUKIT TIMAH FOREST, SINGAPORE

M.D. Sherlock[1], Nick Chappell and Tony Greer[2]
[1]Institute of Environmental and Biological Sciences, Lancaster University, Lancaster, UK
[2]Department of Geography, National University of Singapore, Singapore

ABSTRACT

The spatial distribution of soil hydrological properties and associated flow pathways within a single 0.01 to 10 km^2 catchment are usually poorly defined by typical programmes of point-scale measurements. This is due not only to "measurement uncertainty" caused by instrument error and inadequate spatial sampling but also to "conceptual uncertainty" resulting from a deficiency in the Darcy-Buckingham-Richards description of subsurface flow. This study examines these two sources of uncertainty in the identification of subsurface flow beneath the Bukit Timah forest, Singapore. The two distinct approaches of water-tracing and Darcy-Buckingham calculations are compared. Flow estimates resulting from quasi-steady Darcy-Buckingham calculations were found to be very sensitive to the magnitude and pattern of the saturated hydraulic conductivity, which itself was sensitive to the permeametry technique used. The use of a Hydro-Physics ring permeameter in the estimation of subsurface flows gives rates that are far greater than the mean propagation rates of tagged water though the approach identifies the relative difference between the behaviour of the two slopes studied. Whilst the lumped differences between the two tropical slopes may be identified with the Darcy method, the poor correlation with the absolute velocity and direction of the tracer plume means that catchment or even slope scale simulation using parameters of the Darcy-Buckingham-Richards equation will be highly uncertain.

INTRODUCTION

Most physically-based models of water-flow within variably-saturated catchment soils are based on the Richards equation (see, for example, Beven & Moore, 1992). The spatial patterns of soil parameters or subsurface-pathways used to condition these predictive models at the catchment or even slope scale are, however, typically very limited (Chappell & Ternan, 1992). Furthermore, the validity of the Richards equation (or the Darcy-Buckingham equation in its steady-state form) at slope or catchment scales can be questioned. Dagan (1979) and Germann (1990), for example, demonstrate how the equation's parameters of hydraulic conductivity (K) and moisture release ($\theta\ f(\psi_p)$) and its key variable of capillary potential (ψ_p) can be poor representations of the "effective" behaviour within individual pore-volumes.

Singapore Journal of Tropical Geography, Vol. 16, No. 2 (1995), 197-215

Further slope-scale measurements of subsurface parameters and pathways are therefore valuable to the conditioning of future simulation modelling and in further evaluation of the Darcy-Buckingham-Richards approach itself. Whilst there have been a few slope-scale hydrological research programmes in temperate latitudes (Dunne, 1978; Anderson & Burt, 1990), there is an almost complete dearth of studies within the humid tropics (Bonell & Balek, 1993).

Within the tropics, serious contemporary issues such as the contamination of surface and groundwater resources and flood hazard would benefit from a better understanding of slope-scale hydrological processes. These two issues are key management concerns for the Republic of Singapore, where 45 per cent of Singapore Island is water-supply catchment (Appan, 1992) and pluvial flooding is common (Gupta, 1992).

This study seeks to identify shallow groundwater processes within slope sections of the Jungle Falls catchment, Bukit Timah forest, Singapore Island. Flow-paths are identified using both a Darcy-Buckingham approach and a water-tracing methodology. This combined use of the two techniques may explain why the Darcy-Buckingham-Richards approach has "failed" at other sites. Plot-scale experiments were conducted within an area of lowland dipterocarp rain forest which comprises the Bukit Timah Nature Reserve. Identification of soil-water pathways beneath this rain forest cover may therefore also have relevance to current research on nutrient cycling within tropical soils (Bruijnzeel, 1990).

EXPERIMENTAL SITE

The Jungle Falls catchment is 0.05 km^2 in area and is located on the north-western fringes of the 0.71 km^2 Bukit Timah Nature Reserve, which contains the largest surviving area of primary rain forest on Singapore Island (Fig. 1) (Corlett, 1990). The catchment ranges in altitude from 90 to 164 m. Slope angles are less than 10° on the crest zones, 13° to 20° on the midslopes and up to 30° next to the stream channel. The soils are dystric nitosols of the Rengam series (FAO-Unesco, 1974; Ives, 1977; Rahman, 1992) and overly a granite saprolite which is up to 10 m deep in places (Chatterjea, 1989). The A, B_1, B_2 and B_3 soil horizons are identifiable at depths of approximately 0-10 cm, 10-30 cm, 30-70 cm and >70 cm respectively. The texture of each horizon is presented in Table 1. The soil clays are predominantly kaolinitic (Rahman, 1992).

Mean annual rainfall for the whole of Singapore Island and locally on Bukit Timah is approximately 2,370 mm (Chatterjea, 1989; Fook, 1992). During

TABLE 1. PARTICLE SIZE DISTRIBUTION OF RENGAM SOIL SERIES

DEPTH (cm)	HORIZON	PARTICLE SIZE DISTRIBUTION (%)			TEXTURE (ACCORDING TO U.S.D.A. CLASSIFICATION SCHEDULE)
		Sand	Silt	Clay	
0-10	A	70	2	28	Sandy clay loam
10-30	B_1	61	1	38	Sandy clay
30-70	B_2	57	3	40	Sandy clay
70-160	B_3	55	2	43	Sandy clay

Source: Rahman, 1992.

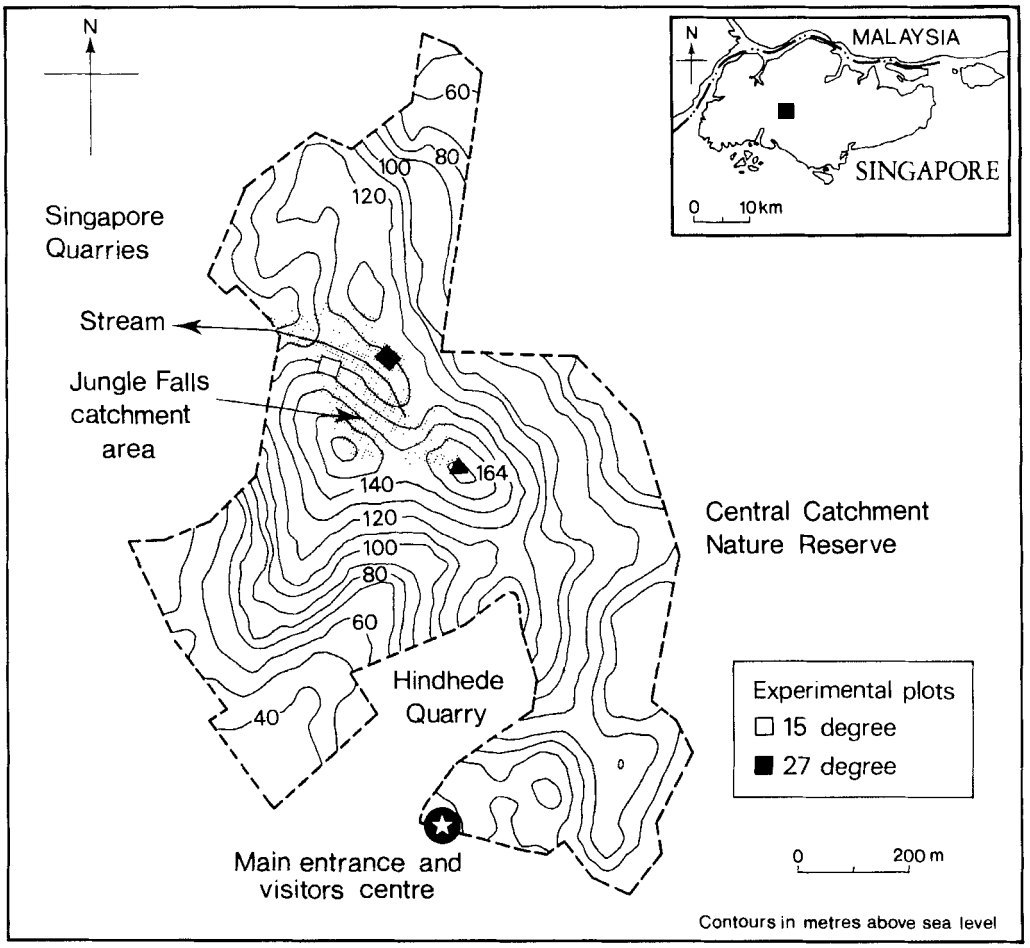

Fig. 1. Location of the Jungle Falls catchment within the Bukit Timah Nature Reserve.

the field study, 15 minute intensities of up to 111 mm hr^{-1} were recorded in the Jungle Falls catchment. Chatterjea (1989) reports that slightly larger 15 minute intensities of 120 mm hr^{-1} on Bukit Timah have a return period of only two years.

EXPERIMENTAL RATIONALE

Within the Jungle Falls catchment two contrasting slope sections with similar vegetation characteristics were instrumented, one very steep at 27° and the other at 15° which is more representative of the average slope within the area. The instrumented section was 5 x 4 m in area and divided into two sub-plots (Fig. 2). One sub-plot comprised vacuum samplers and resistance cells for water-tracing experiments, whilst the adjacent sub-plot was instrumented with arrays of mercury manometer tensiometers. These tensiometer data are used in Darcy-Buckingham calculations of water-flow.

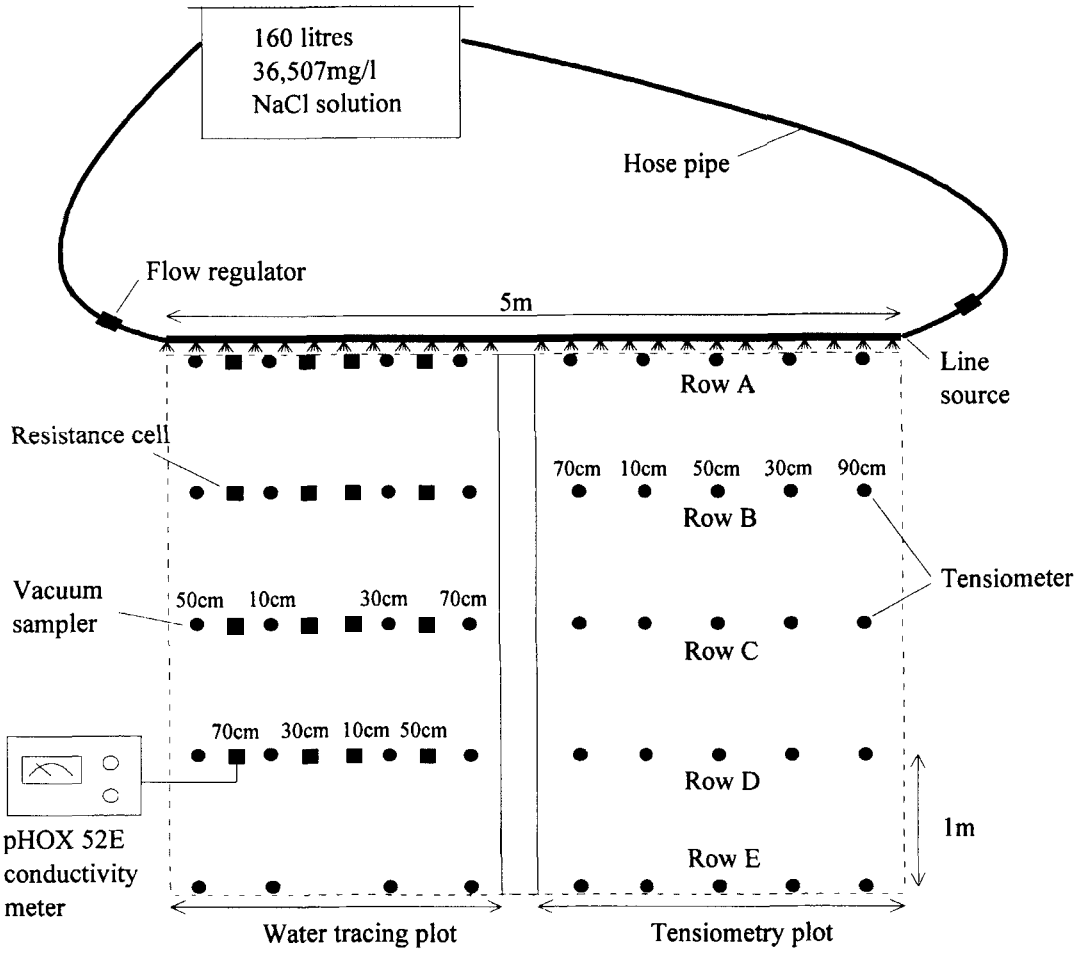

Fig. 2. Schematic representation of the instrumental plot within the Jungle Falls catchment.

Solution of the Darcy-Buckingham equation for soil-water flow

The Darcy-Buckingham equation describes water-flow under quasi-steady, unsaturated (and saturated) soil conditions (Kutilek & Nielsen, 1994). In one dimensional form it can be written as:

$$q = -Kf(\psi_p).d(\psi_g + \psi_p)/L \qquad (1)$$

where q is the macroscopic velocity of water (cm hr^{-1}), $Kf(\psi_p)$ is the hydraulic conductivity as a function of ψ_p which is the capillary potential (cm), ψ_g is the gravitational potential (cm), and L is the length over which the hydraulic gradient (or total potential gradient) is measured (cm).

To estimate the water-velocity under quasi-steady conditions, measurements of the total potential gradient (i.e., $d(\psi_g + \psi_p)/L$) and the "$Kf(\psi_p)$ curve" are needed at each location within

the sub-plot. In this study, the capillary potential (ψ_p) was measured every five minutes within most storm events and daily during intervening periods. Siting several arrays of five tensiometers at depths of 10, 30, 50, 70 and 90 cm within each plot enables the calculation of both vertical and downslope potential gradients. A dumpy-level was used to define the gravitational potential (ψ_g) at each tensiometer location. The shape of the $Kf(\psi_p)$ curve was derived by Millington-Quirk analysis of moisture release data matched to the layer-averaged saturated hydraulic conductivity (after Millington & Quirk, 1959; Jackson *et al.*, 1965). The moisture release data were derived by fitting a bi-cubic spline (J. Dowd, pers. comm.) to pressure plate measurements. Saturated hydraulic conductivity was determined using two contrasting field techniques of "Guelph permeametry" (Reynolds & Elrick, 1985) and "Hydro-Physics ring permeametry" (Chappell & Ternan, in submission).

Downslope and vertical water-flow for each temporal set of tensiometer measurements was calculated by first using the $Kf(\psi_p)$ curves to determine the hydraulic conductivity for each tensiometer reading. Second, the mean hydraulic conductivity for the soil between two vertically or laterally adjacent tensiometers was then found and multiplied by the hydraulic gradient between the same two tensiometers. Data on the saturated hydraulic conductivity were available for the upper 60 cm of the soil profile only. Darcy-based flow estimates for the 50 to 70 cm and 70 to 90 cm layers are therefore approximated with the saturated hydraulic conductivity data collected at a depth of 50 to 60 cm.

Once the downslope and vertical flow from each tensiometer location were found, the effective or resultant velocity and direction (i.e. flow vector) was calculated using:

$$qR = \sqrt{\{qD + qV \cdot \sin \alpha)^2 + (qV \cdot \cos \alpha)^2\}} \quad (2)$$

$$\gamma = \sin^{-1} (qD \cdot \cos \alpha / qR) \quad (3)$$

where qR, qD and qV are the resultant, downslope and vertical fluxes (cm hr^{-1}), α is the slope angle and γ is the angle of the resultant flux, measured from vertically downwards (Fig. 3; after Harr, 1977). In the following discussion, this methodology is simply referred to as the "Darcy-approach".

Line-source electrical water tracing

A water-tracing experiment was conducted with both slope sections. A slug of chemically-conservative, sodium chloride tracer was sprayed on to a 5 m^2 area immediately upslope of each plot for 15 minutes, delivering a depth of 32 mm at a concentration of 36,507 mg $litre^{-1}$ NaCl. High concentrations are necessary because of the considerable dilution of the tracer in such wet tropical soils (*cf.* Hill, 1972).

Movement of the tracer through the profile was monitored using vacuum samplers and modified 'Colman resistance cells' (Colman, 1946). The cells comprise two gold-coated platinum electrodes separated by three sheets of 'Vyon' plastic mesh. They respond instantly to changes in both surrounding soil moisture status and soil-water salinity, and therefore allow rapid tracer breakthrough resulting from "macropore" flow to be observed. In contrast, vacuum samplers fitted with standard 1 or 2 bar air-entry ceramics take six to twelve hours of 0.6 bar vacuum to withdraw sufficient volume for conductivity measurement. To reduce this time, 0.5 bar "high-flow" ceramic tips requiring slightly shorter extraction times of four to six hours were used at Jungle Falls. A portable conductivity meter (pHOX 52e) was used to measure the electrical output of the cells *in situ* and the electrical conductivity of water samples withdrawn from the vacuum samplers. An initial sampling interval of one to five hours was increased to a daily interval approximately 24 hours after the tracer injection. This sampling resolution was sufficiently fine to characterise the breakthrough curves which peaked between one and approximately 10 days after injection.

CONDUCTIVITY IDENTIFICATION

Physically-based modelling of catchment hydrology indicates that the soil's saturated

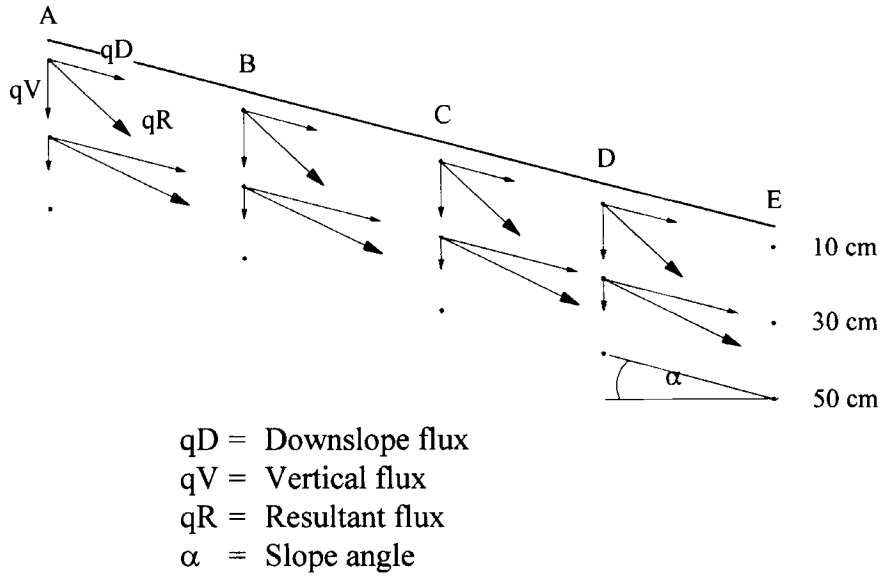

Fig. 3. Calculation of resultant Darcy-derived flows within slope segments of a sub-plot.

hydraulic conductivity (Ks) is the most important parameter governing water-flow. Patterns in soil-water pathways may therefore match patterns in conductivity (Chappell & Ternan, 1992). To allow calculation of water-flow and examination of this hypothesis, a total of 36 Hydro-Physics ring permeametry and 39 Guelph permeametry measurements were taken within the Jungle Falls catchment.

On inspection of the data, the two permeametry methods produced different data distributions. Kolmogorov-Smirnov (K-S) tests indicated that both datasets are highly skewed though to a different degree (Table 1). A fourth root transform was required to normalise the Guelph-derived data and a $\log_{10}$ transform to normalise the ring-based data (Table 2). The data measured by the Guelph permeameter are therefore less skewed than those measured with the ring permeameter.

The Ks datasets both indicate a decrease in conductivity with depth, although the magnitude of the apparent decline again differs between the two (Fig. 4). The measurements derived using the Guelph permeameter indicate that Ks decreases by over three orders of magnitude within the upper 60 cm of the soil profile. In contrast, measurements from ring permeametry suggest a loss of conductivity of slightly more than one order of magnitude over the same depth.

The difference in the statistical and spatial distributions of Ks may be the result of two competing effects. First, borehole methods of permeametry including the Guelph technique are sensitive to smearing of the augured borehole, particularly when undertaken in clayey soils such as those at Bukit Timah (see Table 1). Smearing will obviously reduce the measured Ks value, but may also reduce the skew by having a greater impact on the flow into large soil-pores. The Guelph method incorporates a borehole brushing stage to combat smearing; however, it has been suggested that this is only partially successful (Chappell & Ternan, in submission). Second, ring permeametry is subject to error in the applied boundary condition. Root channels and natural structural cracks that

TABLE 2. KOLMOGOROV-SMIRNOV TEST OF NORMALITY FOR RAW AND TRANSFORMED DISTRIBUTIONS OF Ks DERIVED BY BOTH RING AND GUELPH PERMEAMETRY

DATASET	K-S STATISTIC	SIGNIFICANCE LEVEL
Raw, Ring-based data	0.2995	0.003
Raw, Guelph-based data	0.2439	0.019
Fourth root transform, Ring data	0.1578	0.331
Fourth root transform, Guelph data	0.0981	1.000
Log 10 transform, Ring data	0.1019	1.000
Log 10 transform, Guelph data	0.1685	0.218

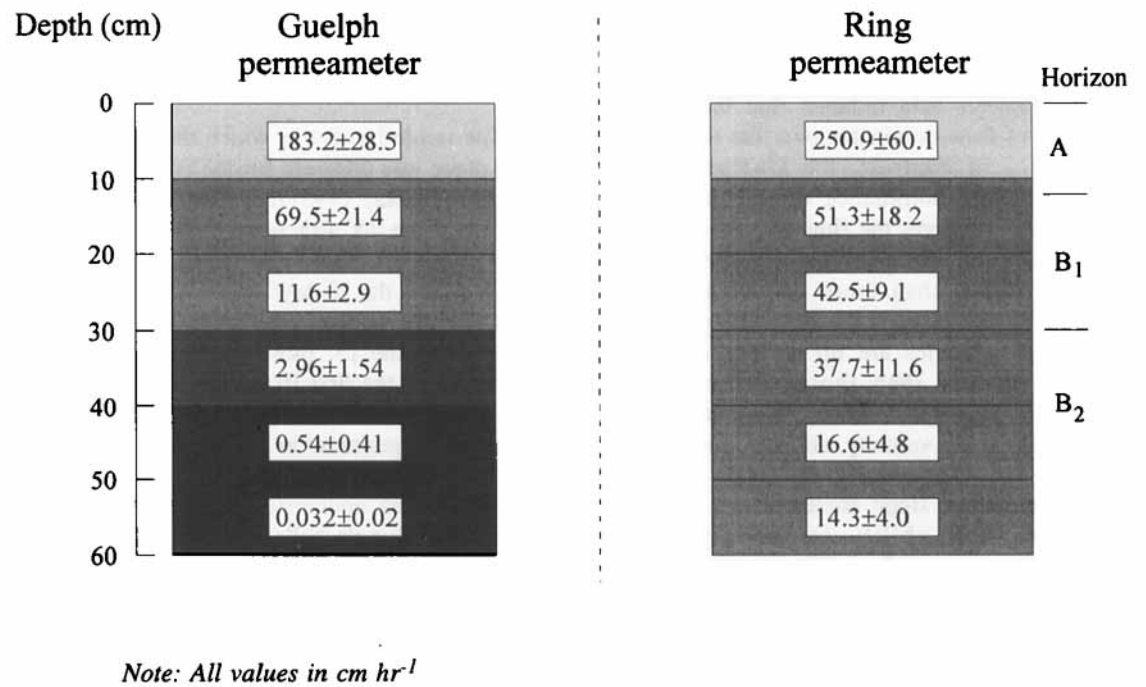

Fig. 4. Comparison of mean saturated hydraulic conductivity values derived using the Guelph and ring permeameters.

extend the whole length of permeameter cores allow very rapid drainage of the applied water. If these large pores are not naturally continuous between soil horizons that have been separated for ring permeametry, then the Ks measured will be an over-estimate.

Using the data collected in the Jungle Falls catchment the impact of the permeametry method on flow estimates is illustrated by using both methods to calculate flow under the same moisture conditions. Moisture conditions within the 15° experimental plot on 23 April 1993 were used for this comparison.

EFFECT OF PERMEAMETRY METHOD ON FLOW-ESTIMATES

The dissimilarity in the resultant direction and magnitude of water flow calculated using data derived from both permeameter techniques is illustrated in Figure 5. The length of the arrows on the velocity plots are proportional to the logarithm of the velocity to allow the whole velocity range to be plotted. The water velocities calculated using ring permeameter data indicate that the vertical component of flow dominates over the downslope component. In contrast, the Guelph-derived data indicate the dominance of the downslope component. Furthmore, the ring-derived velocities within B_1 horizon are approximately one order of magnitude greater than those derived using the Guelph technique. Within the B_2 and B_3 horizon, ring-derived velocities are up to four orders of magnitude greater than those of the Guelph permeametry. Such differences in the calculation of slope-scale water velocity and direction may be larger than the differences likely to be observed with differing soils, slope angles or soil moisture conditions. The ability to identify actual macroscopic water-paths is therefore strongly dependent on the choice of permeametry technique.

Excavation of the augerholes used for the Guelph permeametry clearly showed signs of smearing even after using the recommended pre-test brushing. The ring permeametry results are used therefore within all subsequent Darcy-based calculations.

DARCY-BASED FLOWS IN THE PLOTS

The Darcy-based analysis covers the first 10 days of both tracer experiments. Within the 15° plot, tracer injection began at 12:33 hours on 23 April 1993 and at 14:59 hours on 28 May 1993 in the 27° plot. In both cases this was shortly after the beginning of the respective rainstorms. The hydrometric response to these two rainstorms is presented in Figures 7 and 8. The average Darcy-based flows resulting from these two storms use potential data collected during a period from five minutes after the storm began to twice the duration of the storm. For the 15° plot this period is between 12:33 and 18:35 hours on 23 April 1993 and for the 27° plot between 14:59 and 18:16 hours on 28 May 1993. The response during the initial minutes of each storm when highly unsteady conditions prevailed is excluded to meet the quasi-steady criterion of the Darcy-Buckingham approach. Average flows for the 10 day periods beginning with these three or six hour periods are also calculated. These 10 day periods are comparable with the times of peak for most of the tracer breakthough curves.

The rainfall event in which the tracer injection took place was different for the two plots, with the 27° plot (28 May 1993) receiving 13 per cent of the rainfall of the 15° (23 April 1993) plot. Records from the Turf Club raingauge two km away, indicated that the 10 days following tracer injection were slightly wetter in the 27° plot in comparison with that in the 15° plot (Table 3). Average soil moistures for the first 10 day period of the 27° plot experiment were, however, much higher than those during the experiment in the 15° plot (Fig. 6). The small difference in the Turf Club rainfall totals may be therefore an underestimate of the difference in totals in the Jungle Falls catchment. This may be explained by the localised convective nature of the rainfall in Singapore (Fook, 1992).

Flows in the 15° plot

During the storm of the 23 April 1993, the calculated flow-vectors within the 15° plot varied

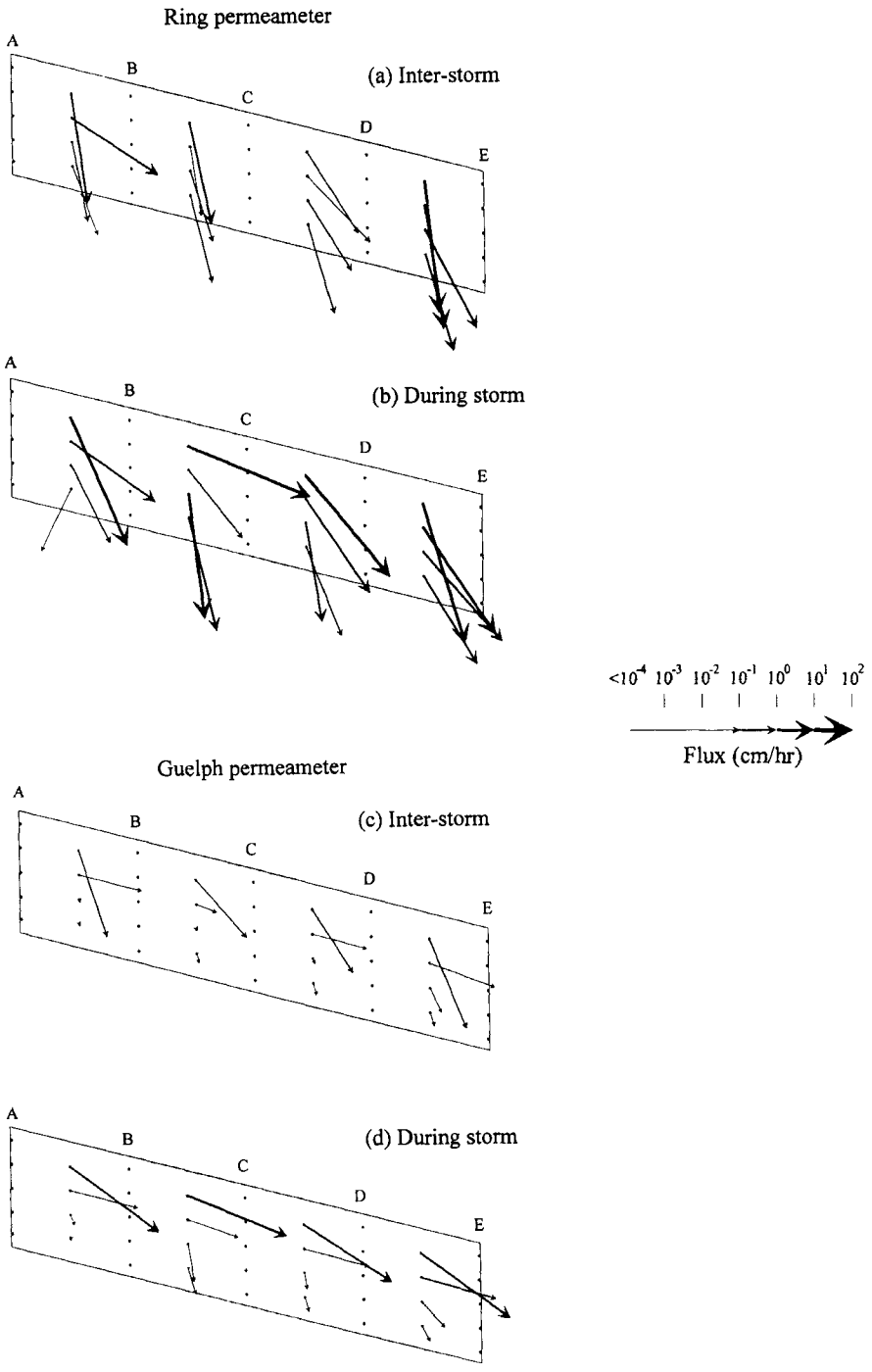

Fig. 5. Comparison of resultant fluxes calculated using the ring and Guelph permeameters in the 15° plot on the 23 April, 1993.

TABLE 3. RAINFALL CHARACTERISTICS DURING THE TRACER TESTS

PLOT	DATA OF TRACER INJECTION	DURATION OF STORM WITH TRACER INJECTION*	RAINFALL OF STORM WITH TRACER INJECTION* (mm)	PEAK RAINFALL INTENSITY DURING STORM WITH INJECTION* (mm hr^{-1})	RAINFALL FOR 10 DAYS AFTER TRACER INJECTION+ (mm)	RAINFALL FOR 20 DAYS AFTER TRACER INJECTION (mm)
15°	23/4/93	3 hr 46 mins	111.7	111.92 (29 min. duration	155	208
27°	28/5/93	1 hr 13 mins	14.4	22.7 (25 min. duration)	183	234

* Storm-based raingauge in the Jungle Falls catchment.
\+ Turf Club rainguage, 2 km east of Jungle Falls.

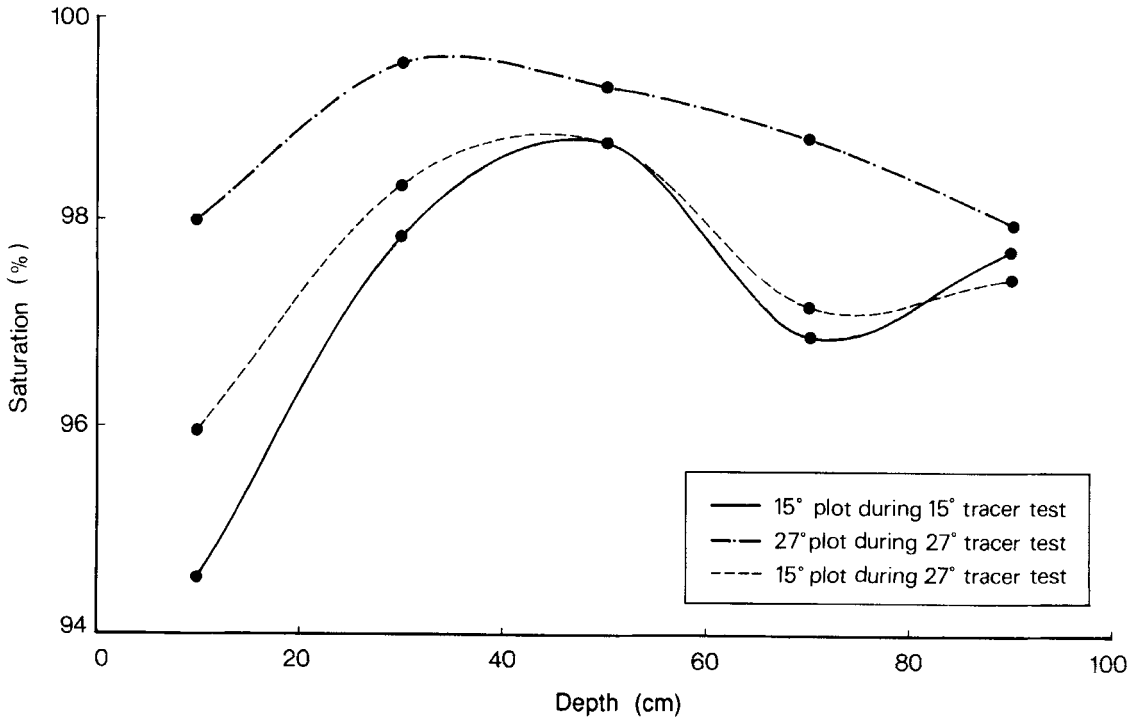

Note: Values of per cent saturation are derived from capillary potential data using the moisture release curves.

Fig. 6. Mean soil moisture content during the initial 10 days of the tracer tests.

considerably, both in time and across the plot (Table 4 and Fig. 7). Flows within the B_2 and B_3 horizons are consistently lower at the same time-step than those within the B_1 though this may be expected given the decline of conductivity with depth. The direction of the resultant flows before rainfall contrasts markedly with those following the onset of rain. Prior to the rain the water-flow is calculated to follow a predominantly vertical direction (Fig. 7, t_1=12:16). After rainfall has commenced, however, rapid lateral movement of water developed within the B_1 horizon (Fig. 6, t_2 to t_5). The resultant direction of flow within the underlying B_2 and B_3 horizons remained relatively unchanged throughout the storm, although some hillslope segments did indicate a minor increase in the downslope flow component.

Flows in the 27° plot

The direction of the flow within the upper segment of the 27° plot was predominantly downslope both prior to and during the storm on the 28 May 1993 (Fig. 8). This greater lateral flow component may be because of steepness of the slope that has accentuated the relatively small hydraulic discontinuities in the profile (see Zaslavsky & Sinai, 1981). The higher soil moisture content may itself be caused by the 27° soil profile being shallower, thus forcing deep subsurface flow to return to the near surface soils.

During the course of the storm, flows at depths of between 20 and 40 cm (B_1 and upper B_2 horizons) increased by two orders of magnitude, in comparison to an increase of only one order of magnitude over the same depth in the 15° plot (Table 5). Within the lower profile of the 27° plot, the average water velocity actually declined during the storm period (Table 5). The wetting front therefore had not reached the lower B_2 (50-70 cm) and B_3 horizons some 1 hour 53 minutes after the start of the storm. A greater lag in the arrival time of a wetting front at this depth may be expected given greater lateral flows within the upper profile.

TABLE 4. MAGNITUDE OF RESULTANT FLOWS IN THE 15° PLOT PRIOR TO (t_1) AND DURING RAINFALL (t_1 TO t_5) ON THE 23 APRIL 1995

DEPTH (cm)	RESULTANT FLOWS (cm hr^{-1})	
	Before Storm (t_1)	During storm (t_2-t_5)+
10-30	0.69-5.25 (2.34)	12.5-60.26 (40.7)
30-50	0.26-7.4 (2.29)	0.21-16.6 (3.71)
50-70	0.21-2.69 (0.95)	0.25-13.18 (2.57)
70-90	0.07-0.63 (0.41)	0.09-5.5 (0.98)

+ For times t_1 to t_5 see Figure 7.
Bracketed numbers indicate mean flux.

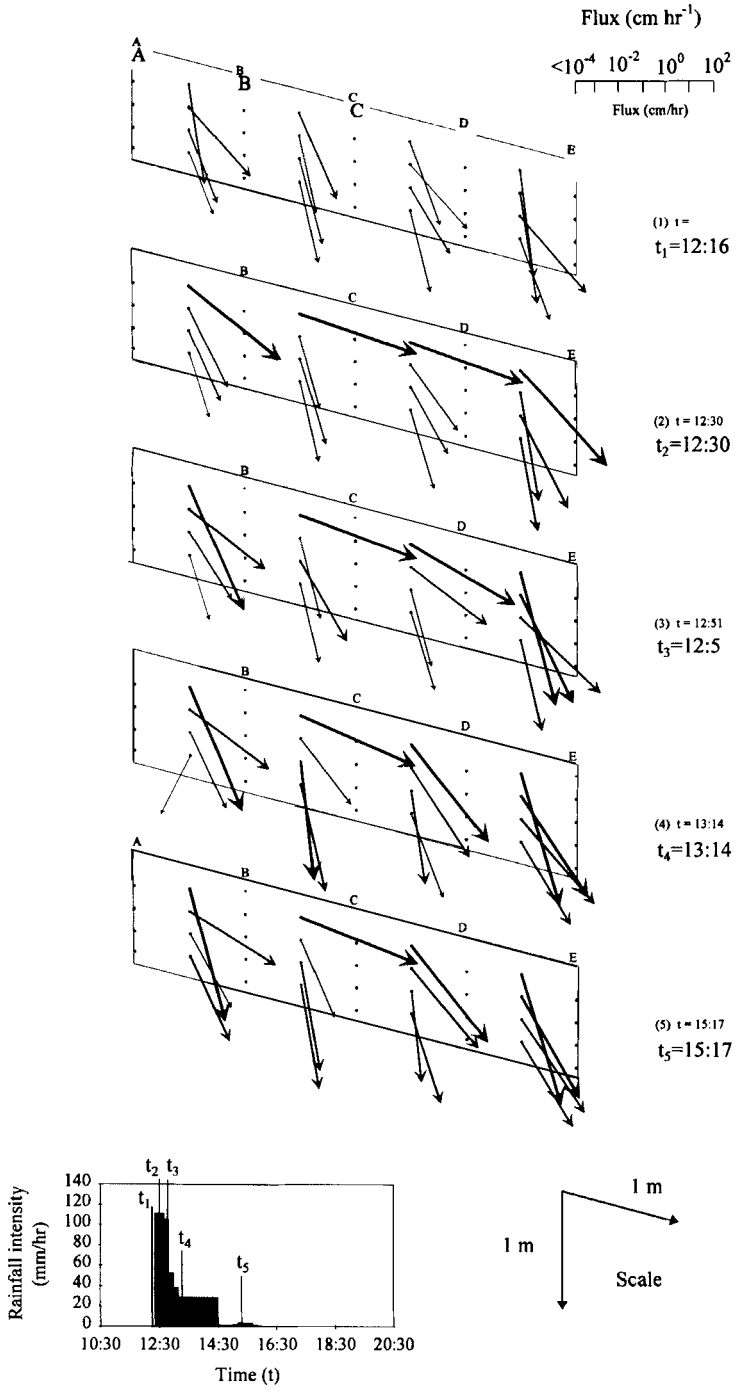

Note: Tracer was injected at 12:33 hours on the 23 April 1993, shortly after the rainfall began at 12.20 hours.

Fig. 7. Magnitude and direction of fluxes in the 15° plot over the storm of tracer injection.

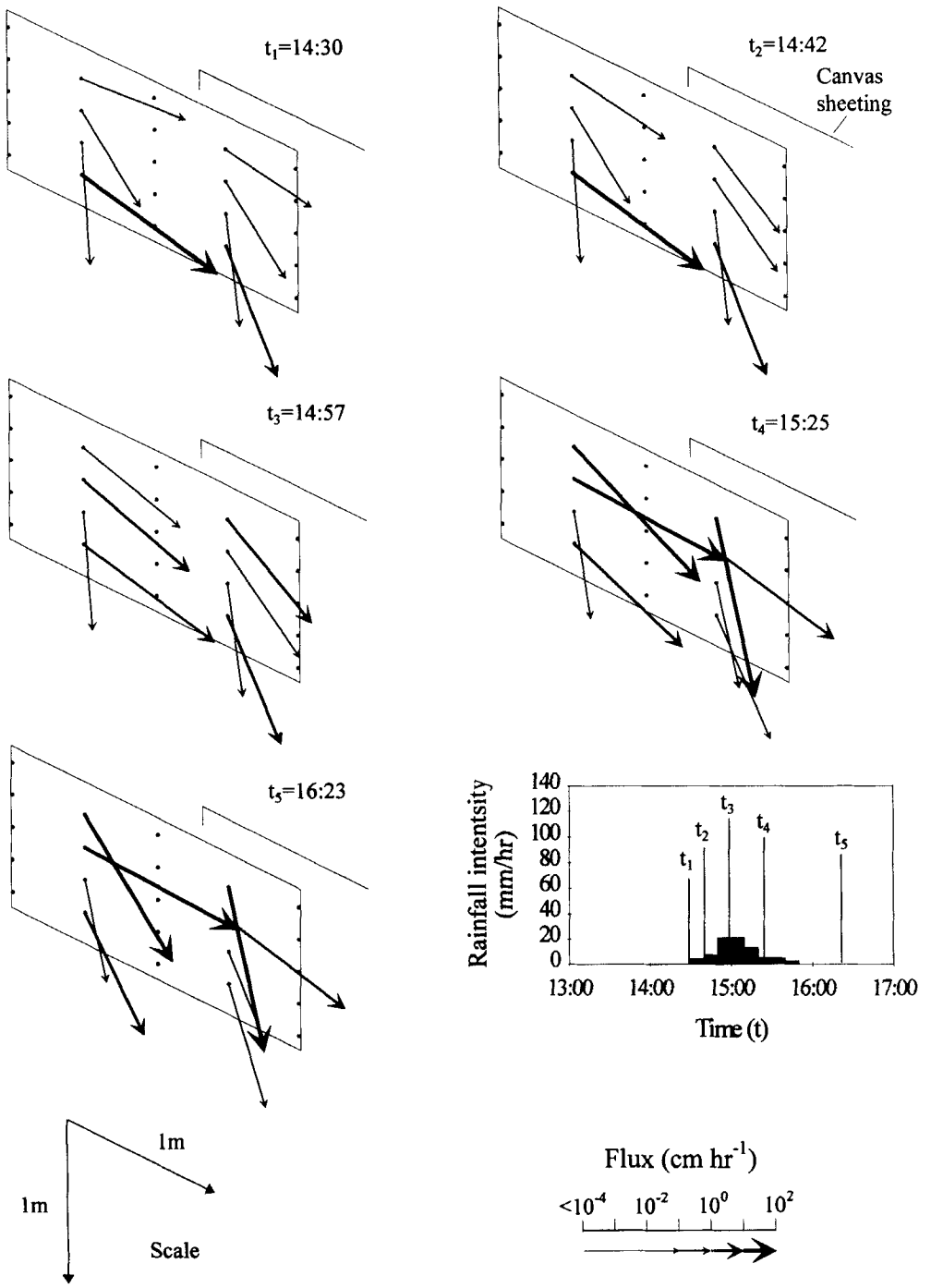

Note: Tracer was injected at 14:59 hours on the 28 May, 1993, shortly after the rainfall began at 14.32.

Fig. 8. Magnitude and direction of fluxes in the 27° plot over the storm of tracer injection.

TABLE 5. CHANGE IN WATER VELOCITY DIRECTLY AFTER CESSATION OF RAINFALL COMPARED WITH VELOCITY PRIOR TO RAINFALL

DEPTH (cm)	CHANGE IN SOIL WATER VELOCITIES AFTER RAINFALL HAS CEASED COMPARED WITH PRE-STORM VELOCITIES (Log pR)	
	15° Plot	27° Plot
10-30	+14.00	+2.21
30-50	+0.92	+2.56
50-70	+0.97	-0.554
70-90	+0.96	-0.912

Values in cm hr^{-1}.
+ and - denote increase and decrease in velocity respectively over the duration of the storm.

TRACER IDENTIFICATION

Tracer sampling paralleled the tensiometer monitoring during the two periods beginning on the 23 April and 28 May 1993. Effective pore-water velocities for the initial appearance, peak and mean concentration of the tracer were calculated from each tracer sampling point (see Fig. 2) by dividing the times on the breakthrough curves by distance traveled.

Two sampling methods were used: resistance cell monitoring and vacuum extraction, and these were shown to give different breakthrough curves. Following analysis of these curves, the resistance cells indicate greater pore-water velocities for both the initial arrival and peak concentration of the tracer, in comparison with the vacuum samplers (Table 6). In particular, initial breakthrough velocities at all depths within the 27° plot are one to three orders of magnitude greater when measured by the resistance cells in comparison with the adjacent vacuum samplers. The difference is probably caused by the resistance cells being more sensitive to water movement through the active pore space or "macropores", in comparison with the vacuum samplers which extract water from all pores. This may imply that the resistance cells can be used to characterise the response of the "macropores", while the vacuum sampling better characterises flow within the soil peds.

TRACER PROPAGATION IN THE 15° AND 27° PLOTS

The dominant direction of tracer migration within both plots is vertical (Fig. 9). Considerably attenuated breakthroughs are discernible at the Row B samplers (i.e., one metre downslope of the injection) within the 27° plot, but cannot be identified at the same slope location within the 15° plot (Fig. 9). Greater lateral flow is therefore observed within the 27° plot.

Propagation rates of the peak tracer concentration can be compared between the two sites, given that both had the same 15 minutes of tracer injection. Vacuum sampler measurements suggest that the velocity of the peak concentration within the B_1 and B_2 horizons of the 27° plot was two to three orders of magnitude greater than that apparent at

TABLE 6. INITIAL BREAKTHROUGH AND PEAK TRACER VELOCITIES DERIVED USING BOTH RESISTANCE CELLS AND VACUUM SAMPLERS

	DEPTH (cm)	INITIAL BREAKTHROUGH VELOCITY (cm hr^{-1})	VELOCITY OF PEAK OF TRACER (cm hr^{-1})	MAGNITUDE OF PEAK (mg l^{-1} NaCl)
15° plot				
Cells	10	85.72	33.30	7,124.6
	30	0.12	0.08	779.3
	50	0.09	0.05	156.8
	70	0.72	<0.05	>816.9
Samplers	10	4.20	0.023	420.1
	30	12.59	0.077	882.1
	50	0.41	<0.036	>451.8
	70	0.72	0.130	1,113.5
27° plot				
Cells	10	119.94	119.04	4,597.0
	30	-	-	-
	50	53.56	<0.87	>42,793.0
	70	520.83	<0.22	>2,874.0
Samplers	10	4.51	4.51	8,874.0
	30	13.53	1.37	18,943.0
	50	22.55	2.28	17,078.0
	70	31.57	<0.22	>5,367.0

the same depth within the 15° plot (Table 6). The greater velocity within the 27° plot may be due to a higher hydraulic conductivity. The recession from the peak concentration in the 27° plot is considerably faster than in the 15° plot (Figs. 9a and 9c). This indicates that the mean tracer velocity in the 27° plot is higher than that in the 15° plot. Again this may be due to a higher hydraulic conductivity.

The peak concentration observed within the B_1 and B_2 horizons of the 15° was one to two orders of magnitude less than both the initial tracer solution (36.507 mg $litre^{-1}$ NaCl) and the peak concentration observed in the same horizon of the 27° plot (Table 6 and Fig. 9). Lower breakthrough concentrations within the 15° plot could be due to loss from the profile in "soil pipes", though only limited visual evidence for these features is observed within the catchment (e.g., Chatterjea, 1989) or a slower release of the tracer from the topsoil (A horizon) which is evidenced by the more dispersed breakthrough curves (Fig. 9a).

DARCY-DERIVED VERSUS TRACER-DERIVED FLUX

To allow comparison of the Darcy-derived flow estimates with those derived from the tracer breakthrough curves, the macroscopic velocities from Darcy-based calculations (q, cm hr^{-1})

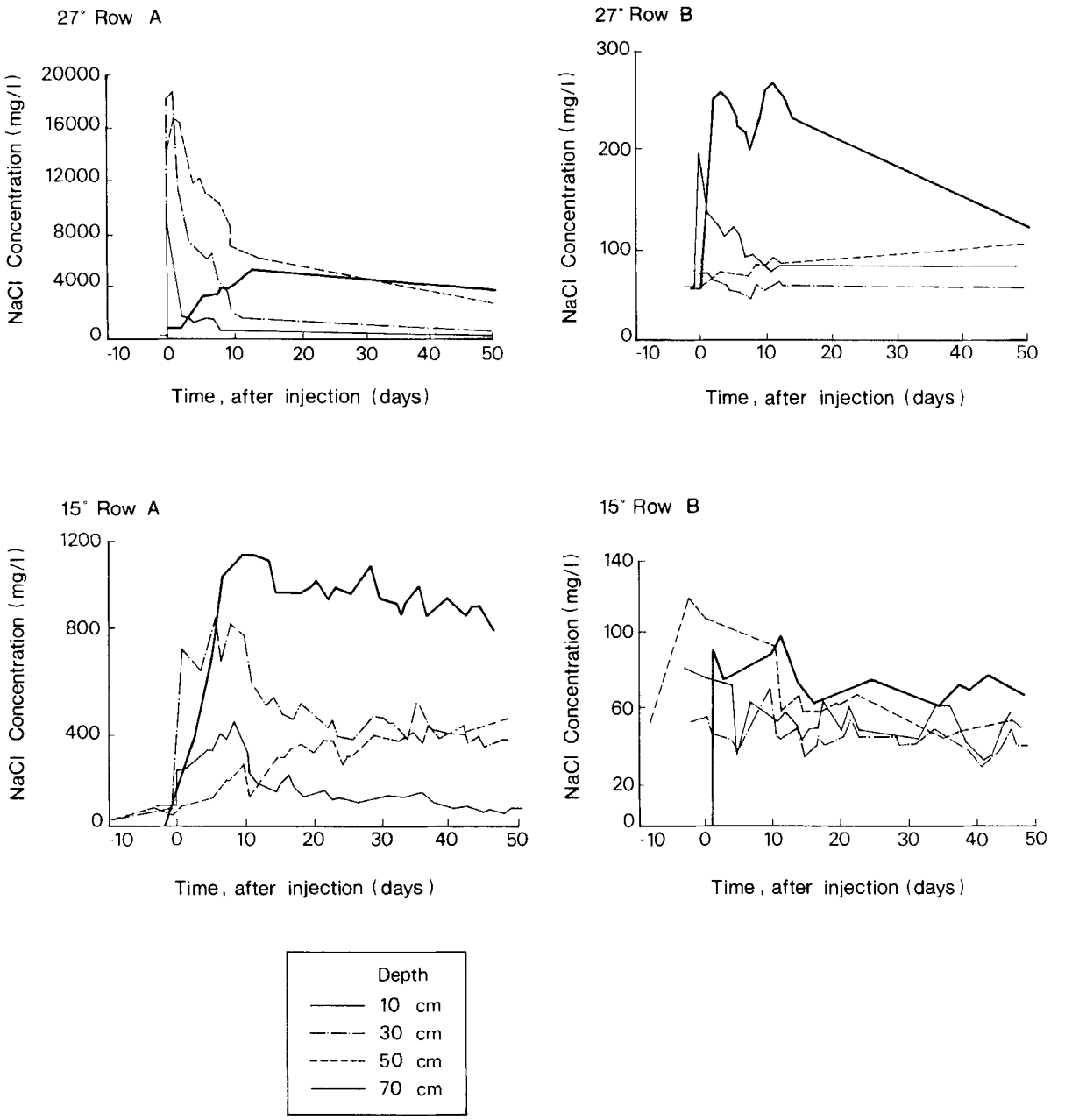

Fig. 9. Breakthrough curves measured at the Row A and Row B vacuum samplers in the 27° and 15° plots.

were converted to mean pore-water velocities (V_{DARCY}, cm hr^{-1}) through division by the porosity (η, cm^3 cm^{-1}), that is:

$$V_{DARCY} = q/\eta \quad (4)$$

The porosity was determined as part of the moisture release analysis and was 0.49 cm^3 cm^{-3} at 10 cm, 0.42 cm^3 cm^{-3} at 30 cm, and 0.37 cm^3 cm^{-3} at 50 cm, 70 cm and 90 cm depth. The value of V_{DARCY} presented in Table 7 are depth-specific averages for the three or six hour and 10 day integration periods.

Where input of a chemically-conservative tracer to a soil is continuous, its mean travel time (T-MEAN) will be half the time it takes for the concentration (C) at a downstream sampling point to approach the input concentration (Co). Division of the travel distance by this mean travel time then gives the mean pore-water velocity ($V_{T\text{-}MEAN}$). Where only a short pulse of tracer is applied to a soil, then $V_{T\text{-}MEAN}$ can be estimated by either (i) extrapolating the rising limb of the breakthrough curve to 0.5Co, or by (ii) extrapolating the recession limb of the breakthrough curve until it integrates at least 95 per cent of the applied tracer mass, when the centroid of the curve then gives T-MEAN. For the Bukit Timah data, approximate values of $V_{T\text{-}MEAN}$ were derived from poorly constrained extrapolations of both the rising and recession limbs of breakthrough curves from the Row A vacuum samplers (see Fig. 9). These values of $V_{T\text{-}MEAN}$ are presented in Table 7 together with the more accurate tracer velocities relating to the first arrival at the highly response, Row A resistance cells ($V_{INITIAL}$) and the peak concentrations recorded by the Row A vacuum samplers (V_{PEAK}).

Table 7 shows that both the 10 day Darcy-derived and mean tracer velocities (recession-based) at all depths are approximately one order of magnitude larger in the 27° plot than in the 15° plot. These data similarly show little vertical pattern in the flows. The marked differences in Darcy-based flow behaviour at one point in space and time with a single plot (Figs. 7 and 8) therefore average out to give horizon-specific flows that are similar throughout the profile. If Darcy-based flows had been derived from the Guelph permeametry rather than ring-based data they would have indicated a marked decline in velocity with depth (see Figs. 4 and 5). There is therefore some support for the use of the Hydro-Physics ring permeametry technique in preference to the Guelph method.

Whilst the "pattern" of flow may be similar between the Darcy/ring and tracer approaches, the magnitude of the velocities are, however, very different. The Darcy/ring-based flows are two orders of magnitude faster than the mean tracer migration rates. The values of V_{DARCY} and $V_{T\text{-}MEAN}$ should be similar, theoretically. This may indicate that the instruments used within Darcy approach are more sensitive to the "local macropore system" rather than the bulk properties. As the calculations are most sensitive to the saturated hydraulic conductivity (Ks), then it would imply that the measured Ks values are more representative of the "local macropore system" rather than the bulk system.

Within the B_2 and B_3 horizons of the 15° plot, the Darcy-based flows (V_{DARCY}) are even larger than those associated with the initial breakthrough of the tracer ($V_{INITIAL}$). This result is consistent with the resistance cells within the 15° plot failing to identify point concentrations representative of the tracer plume, due perhaps to the presence of pronounced preferential flow or even "pipeflow".

CONCLUSION

In summary, Darcy-based calculations of flow magnitude and direction are very sensitive to measurements of the saturated hydraulic conductivity which in turn are sensitive to the measurement technique. The use of the Hydro-Physics ring permeameter in the estimation of subsurface flows gives rates that are far greater than mean propagation rates of tagged water, though the approach identifies the relative difference between the behaviour of the two slopes studied.

Whilst the lumped differences between the two tropical slopes may be identified with the Darcy method, the poor correlation with absolute velocity and direction of the tracer plume means that

TABLE 7. PORE-WATER VELOCITIES DERIVED FROM (1) DARCY-BASED CALCULATIONS AVERAGED OVER 12:33 TO 18.35 HOURS IN 15° PLOT AND 14:59 TO 18:16 HOURS IN THE 27° PLOT, (2) DARCY-BASED CALCULATIONS AVERAGED OVER THE 10 DAYS FOLLOWING TRACER INJECTION, (3) INITIAL TRACER ARRIVAL AND PEAK CONCENTRATION BASED ON ROW A INSTRUMENTS AND (4) MEAN TRACER VELOCITY, DERIVED BY EXTRAPOLATION OF THE ROW A BREAKTHROUGH CURVES

DEPTH FOR DARCY ANALYSIS (cm)	(1) DARCY-DERIVED V_{DARCY} FROM INTEGRATION OF TWICE STORM (cm hr^{-1})	(2) DARCY-DERIVED V_{DARCY} FROM 10 DAY INTEGRATION (cm hr^{-1})	DEPTH FOR TRACER ANALYSIS (cm)	(3a) $V_{INITIAL}$ FROM INITIAL TRACER ARRIVAL (RESISTANCE CELLS) (cm hr^{-1})	(3b) V_{PEAK} FROM TRACER PEAK (VACUUM SAMPLERS) (cm hr^{-1})	(4a) $V_{T\text{-}MEAN}$ AT 0.5C/CO FROM RISING LIMB (cm hr^{-1})	(4b) $V_{T\text{-}MEAN}$ AT 0.5C/CO FROM RECESSING LIMB (cm hr^{-1})
27° Plot							
20-30	35.3	43.9	10	119	4.51	2.0	0.2
30-50	42.7	33.6	30	-	1.37	0.2	0.3
50-70	1.04	17.5	50	53.6	2.28	0.8	0.2
70-90	8.13	22.2	70	520	0.22	0.1	-
15° Plot							
20-30	118	10.6	10	85.7	0.023	0.001	0.04
30-50	15.2	2.24	30	0.12	0.077	0.01	0.04
50-70	7.24	2.30	50	0.09	0.036	0.01	-
70-90	5.61	1.42	70	0.72	0.136	0.05	0.06

catchment or even slope scale simulation using parameters of the Darcy-Buckingham-Richards equation would be highly uncertain.

ACKNOWLEDGEMENTS

The authors are grateful to the National Parks Board of Singapore for their kind permission to work in the Bukit Timah Nature Reserve, to the park rangers for their help and co-operation and to the Singapore Meteorological Service for the Turf Club rainfall data. Financial support was provided by the Natural Environment Research Council studentship grant GT4/AAPS/28 and the Environmental Science Division, Lancaster University.

REFERENCES

Anderson, M.G. & Burt, T.P. (eds.) (1990) *Process Studies in Hillslope Hydrology*, Chichester: John Wiley & Sons.

Appan, A. (1992) 'Control of water quality in Singapore', in A. Gupta & J. Pitts (eds.), *Physical Adjustments in a Changing Landscape*, Singapore: Singapore University Press, 374-88.

Beven, K.J. & Moore, I.D. (1992) *Terrain Analysis and Distributed Modelling in Hydrology*, Chichester: John Wiley & Sons.

Bonell, M. & Balek, J. (1993) 'Recent scientific developments and research needs in hydrological

processes of the humid tropics', in M. Bonell, M.N. Hufschmidt & J.S. Gladwell (eds.), *Hydrology and Water Management in the Humid Tropics*, U.K.: Cambridge University Press, 167-260.

Bruijnzeel, L.A. (1990) *Hydrology of Moist Tropical Forests and Effects of Conversion: A State of Knowledge Review*, Paris: UNESCO.

Chappell, N.A. & Ternan, J.L. (1992) 'Flow-path dimensionality and hydrologic modelling', *Hydrological Processes*, 6, 327-45.

Chappell, N.A. & Ternan, J.L. (in submission) 'Ring permeametry: design, operation and error analysis', *Water Resources Research.*

Chatterjea, K. (1989) 'Surface wash: the dominant geomorphic process in the surviving rain forest of Singapore', *Singapore Journal of Tropical Geography*, 10, 95-109.

Colman, E.A. (1946) 'The place of electrical soil moisture meters in hydrological research', *Transactions of the American Geophysical Union*, 27, 847-53.

Corlett, R.T. (1990) 'Flora and reproductive phenology of the rain forest at Bukit Timah, Singapore', *Journal of Tropical Ecology*, 6, 55-63.

Dagan, G. (1979) 'The generalisation of Darcy's Law for nonuniform flows', *Water Resources Research*, 15, 1-7.

Dunne, T. (1979) 'Field studies of hillslope flow processes', in M.J. Kirkby (ed.), *Hillslope Hydrology*, Chichester: John Wiley & Sons, 227-93.

FAO-UNESCO (1974) *Soil Map of the World: Volume I, Legend*, Paris: Unesco.

Fook, F.S. (1992) 'Some aspects of the hydrometeorology of Singapore', in A. Gupta & J. Pitts (eds.), *Physical Adjustments in a Changing Landscape*, Singapore: Singapore University Press, 215-40.

Germann, P.F. (1990) 'Macropores and hydrologic hillslope processes', in M.G. Anderson & T.P. Burt (eds.), *Process Studies in Hillslope Hydrology*, Chichester: John Wiley & Sons, 327-63.

Harr, R.D. (1977) 'Water flux in soil and subsoil on a steep forested slope', *Journal of Hydrology*, 33, 37-58.

Hill, R.D. (1972) 'Soil moisture under forest, Bukit Timah Nature Reserve, Singapore', *Gardens Bulletin*, XXVI.

Ives, D.W. (1977) 'Soils of the Republic of Singapore', *New Zealand Soil Survey Report 36*, New Zealand: New Zealand Soil Bureau.

Jackson, R.D., Reginato, R.J. & Van Bavel, C.H.M (1965) 'Comparison of measured and calculated hydraulic conductivities of unsaturated soils', *Water Resources Research*, 1, 375-80.

Kutilek, M & Nielsen, D.R. (1994) *Soil Hydrology*, Germany: Catena Verlag.

Millington, R.J. & Quirk, J.P. (1959) 'Permeability of porous media', *Nature*, 183, 337-38.

Rahman, A. (1992) 'Soils of Singapore', in A. Gupta & J. Pitts (eds.), *Physical Adjustments in the Changing Landscape*, Singapore: Singapore University Press, 144-89.

Reynolds, W.D. & Elrick, D.E. (1985) 'In situ measurements of field-saturated hydraulic conductivity, sorptivity, and the a-parameter using the Guelph Permeameter', *Soil Science*, 140, 292-302.

Zaslavsky, D. & Sinai, G. (1981) 'Surface hydrology: V In-surface transient flow', *Journal of the Hydraulics Division*, Proceedings of the American Society of Civil Engineers, 107, 65-93.